

6 Degree of Freedom Shock and Vibration: Testing and Analysis

Dr. Brian Owens, Dr. Gregory Tipton, and Matthew McDowell

Analytical Structural Dynamics Department

Sandia National Laboratories[†]

Albuquerque, New Mexico, U.S.A.

ABSTRACT

Six degree of freedom (DOF) shock and vibration testing provides an avenue for improved mechanical qualification of a system or component. Six DOF testing allows for application of a test input that is more representative of actual operational environments. Thus, 6 DOF testing allows for a more meaningful stress state to be excited in a test article. Furthermore, 6 DOF analysis should be considered as a critical companion to 6 DOF testing. 6 DOF analysis is an invaluable tool to improve 6 DOF testing methodologies and recover unmeasured quantities (*i.e.* stress) from associated test inputs. This paper presents a combined experimental and analytical study of 6 DOF shock and vibration. The theory of 6 DOF analysis is presented, important considerations are discussed, and key differences between traditional single-axis and 6 DOF testing and analysis approaches are highlighted.

INTRODUCTION

Mechanical qualification of a system or component relies primarily on shock and vibration testing using a series of inputs that are derived from the environments a system or component will be exposed to throughout its life-cycle. The majority of test specifications can be applied using shaker tables which cover a reasonable amplitude and frequency band. Conventional “shakers” are limited to controlling input in a single axis and a number of widely accepted test methodologies have been developed for single axis or 1 degree of freedom (1 DOF) testing [1-3]. These methodologies apply test inputs sequentially in three orthogonal axes in a coordinate system local to the test article. The inherent assumptions in this methodology are that a series of single axis inputs will excite a stress state similar to those in an actual operating environment and that enough conservatism is present in the input specification to account for the higher stress levels that are likely to exist in a true operational environment with multi-axis input. The first assumption can lead to important failure modes being missed as a result of test methodology, exposing a qualification program to undue risk. The second assumption can lead to overly conservative designs that are lacking in performance. Indeed, previous efforts have examined the differences in test article response/performance during single and multi-axis testing [4-8].

The advent of six degree of freedom (6 DOF) shaker tables allows for significant improvements in shock and vibration testing. Multi-axis measurements of an operational environment can be employed in derivation of multi-axis inputs, thereby improving the accuracy of test specifications that excite representative stress states and failure modes in a test article. Thus, 6 DOF testing and associated test specifications can increase performance by reducing conservatism in designs, as well as reducing risk in qualification programs. Furthermore, while the “in-axis” input of a single-axis test can be well controlled, the “off-axis” (two translational DOFs and three rotational DOFs) inputs

[†] Sandia National Laboratories is a multi-program laboratory managed and operated by Sandia Corporation, a wholly owned subsidiary of Lockheed Martin Corporation, for the U.S. Department of Energy National Nuclear Security Administration under Contract DE-AC04-94AL85000.

are uncontrolled and largely governed by shaker hardware dynamics. It should be noted that in general, off-axis inputs can be significant and potentially excite significant dynamics in a test article. Therefore, 6 DOF testing not only allows for a more representative, multi-axis test environment to be applied to a test article, but also allows for off-axis inputs to be controlled and minimized for traditional single-axis test methodologies.

Although previous work has focused on the advantages and implementation of multi-axis/6 DOF testing [9-14], 6 DOF shock and vibration analysis has received much less consideration. Analytical studies are an invaluable companion to shock and vibration testing. Modeling in the form of pre-test predictions can inform test design and highlight potential issues in a test plan. Post-test predictions are also valuable for model updating, but require an accurate characterization of test inputs and test hardware. Post-test analysis can also predict unmeasured quantities to supplement localized accelerometer or strain gauge measurements. Such predictions might include accelerometer or strain measurements at un-instrumented locations, but can also include detailed stress predictions and forces at interfaces/joints. These predictions are extremely valuable for understanding failure modes and supporting design evolution.

This paper examines 6 DOF shock and vibration from both an experimental and analytical perspective. First, a simple test article is presented along with a companion finite element model. The experimental setup for 1 DOF and 6 DOF vibration testing are discussed, and the derivation of 6 DOF inputs from test data is presented and important considerations are highlighted. The development of a general, automated approach to aid in obtaining 6 DOF inputs for modeling efforts is also discussed. Analytical predictions are made using measured test data to derive 6 DOF inputs for random vibration analysis, and post-processing of stresses from a random vibration simulation highlights differences in stress state under 1 and 6 DOF test inputs. A similar study is conducted using measured shock data from an operational environment to synthesize a 6 DOF input for shock modeling of a component. A comparison of stress state and magnitude is made between this 6 DOF shock input and a single-axis test specification of the environment. Finally, the findings of this work are summarized and conclusions are made.

CONFIGURATION

The hardware configuration considered in this study is the bolted aluminum structure shown in Figure 1. The structure is “can like” with an outer diameters of 6.65”, hollow interior, and moderate wall thickness (3/8”). The bottom piece of the can has a flange for mounting to a shaker table or adapter plate. The top piece of the can has a bolted interface to the lower piece through a series of 36 radial bolts. A cylindrical plate was also bolted to the top of the structure for added mass. The structure has an 8”x8” footprint and height of 10”.

The finite element model of this configuration is shown in **Error! Reference source not found.** The radial interface of the upper and lower piece is modeled through tied constraints at the interface of the upper and lower can. All other bolted connections are modeled using a combination of rigid elements and springs to simulate bolt stiffness at the interface. No model correlation was performed on the current model, but recent work has examined modal correlation of this test article [15]. Nevertheless, the current model is adequate for gaining insights into the differences 1 and 6 DOF testing have on unmeasured responses (stress distributions) of a test article. The finite element mesh has approximately 281k nodes and 267k hexahedral elements.

The base of the article is affixed to a large “seismic” mass by means of rigid bar elements. This arrangement mimics the boundary condition of attaching the test article to a shaker table and is a standard analysis practice. The seismic mass will be used to apply input for vibration and shock analysis. The elastic modes of the model are shown in Figure 3. First bending and axial modes of the structure are around 0.7 kHz and 1.8 kHz respectively. Higher

ovaling and top plate modes are predicted around 2.8 kHz. All calculations presented for this study were performed using the Sierra Mechanics code suite developed by Sandia National Laboratories [16,17].

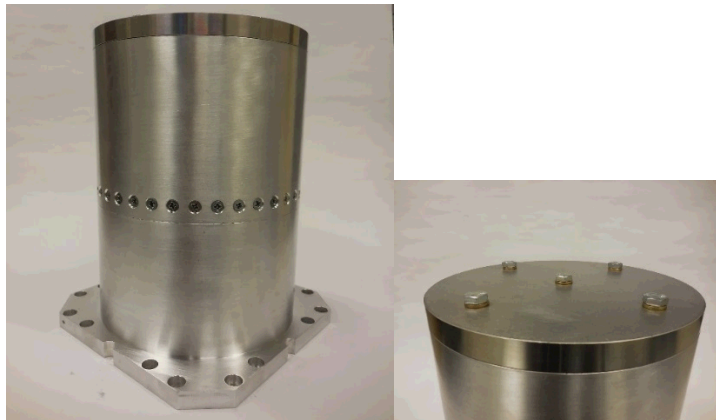


Figure 1 – Photographs of test article.

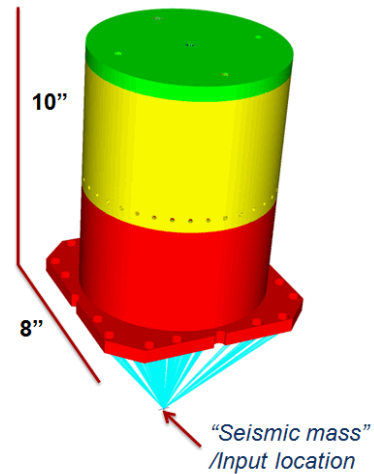


Figure 2 – Finite element model of test article.

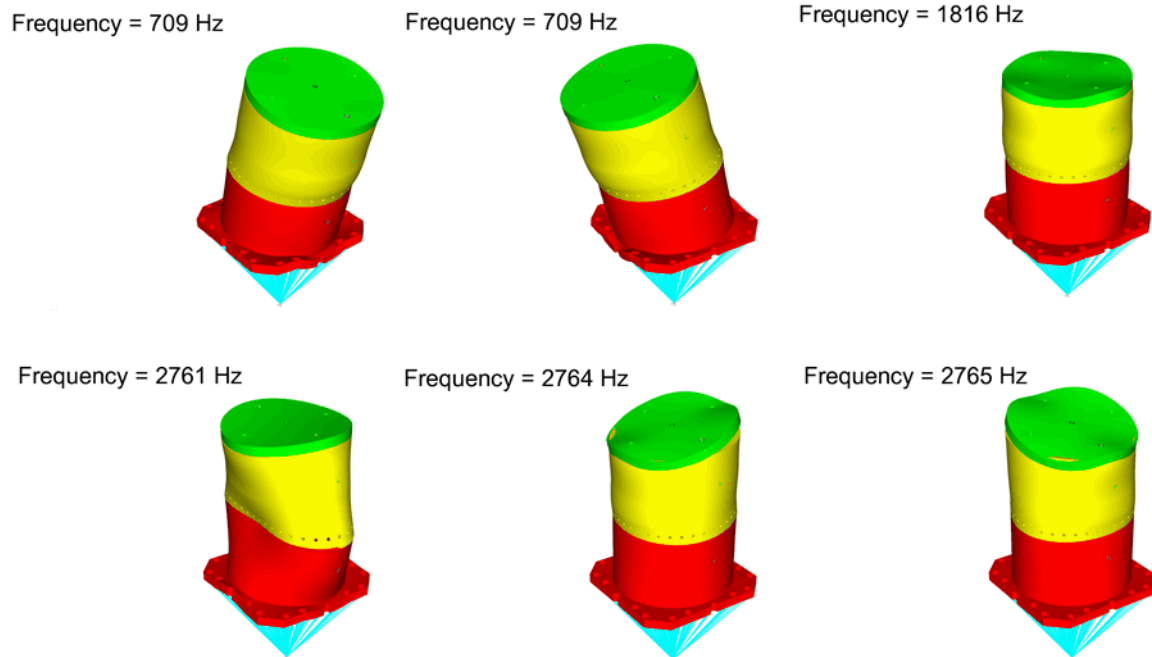


Figure 3 – Predicted elastic mode shapes of test article affixed to seismic mass.

EXPERIMENTAL PROCEDURE

Testing of the structure was performed on both a uniaxial shaker (Unholtz-Dickie T2000) and a 6 DOF Shaker (Team Tensor TE6-900). The 6 DOF shaker setup is shown in Figure 4. Tri-axial accelerometers were placed at multiple locations to better characterize the actual translational and rotational inputs and time histories were acquired. The placement of the accelerometers can be seen in Figure 5. The four accelerometers attached to the base allowed for a thorough characterization of the actual input into the test article. Derivation of the model input using the data from these accelerometers is described in the next section below.

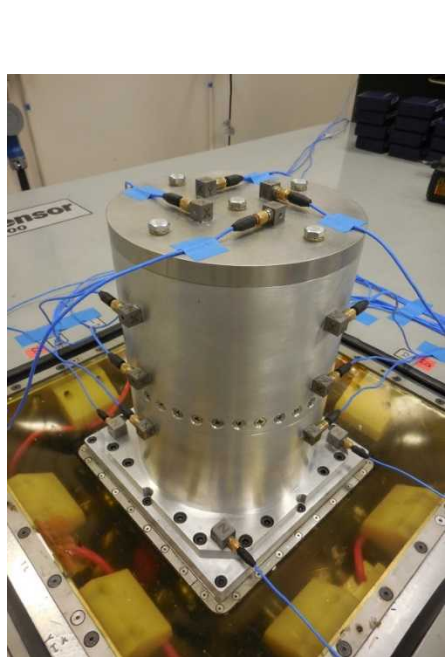


Figure 4 – 6 DOF experimental setup.

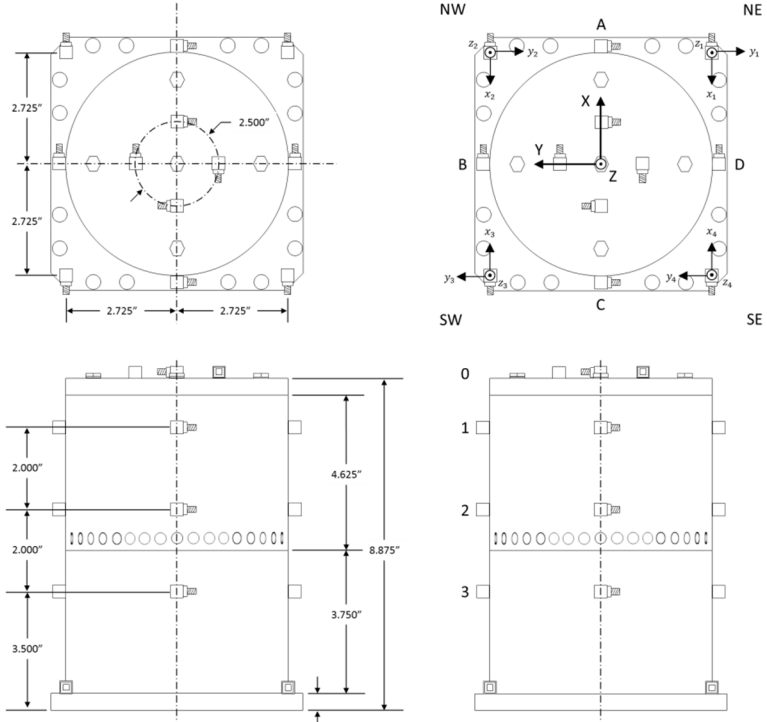


Figure 5 – The basic layout and placement of accelerometers on the test article.

The four accelerometers attached to the base were used for control in the 6 DOF tests. Only a single in-axis channel from these four gauges was used to control the 1 DOF test. Three tests were run on the 6 DOF shaker and one on the 1 DOF shaker. The first of the three 6 DOF tests was performed in an attempt to replicate the 1 DOF shaker test. It provided full level inputs in the axial direction (Z) only. The second was performed to provide full level inputs in all three translational axes without rotations (X, Y, and Z). The third test provided full level inputs and rotations. All of the tests were controlled from 20 Hz to 2 kHz. The specific levels are annotated in Table I.

Table I - Vibration test specifications.

Test	PSD Acceleration Level (20Hz - 2kHz)					
	X-axis (g ² /Hz)	Y-axis (g ² /Hz)	Z-axis (g ² /Hz)	rZ ((g/in) ² /Hz)	rX ((g/in) ² /Hz)	rY ((g/in) ² /Hz)
Z (1DOF)	N/A	N/A	0.001	N/A	N/A	N/A
Z (6DOF)	0.0001	0.0001	0.001	6.73E-6	6.73E-6	6.73E-6
XYZ (6DOF)	0.001	0.001	0.001	6.73E-7	6.73E-7	6.73E-7
XYZrXrYrZ (6DOF)	0.001	0.001	0.001	6.73E-5	6.73E-5	6.73E-5

DERIVATION OF 6 DOF MODEL INPUT

Input for the finite element model was derived from acceleration time histories measured on the base of the test article. These measurements were taken for both the single-axis shaker testing and the 6 DOF-shaker testing. To determine the model inputs, the location of all the accelerometers $\vec{x}^{(i)}$, the location of the “seismic mass”, $\vec{x}^{(0)}$, used as the input location for the loads, as well as the measured accelerations, $\vec{a}^{(i)}(t)$, are required. A standard technique in structural dynamics modeling of base-driven shaker tests is to drive the model with random vibration inputs at a single base node. A large mass (“seismic mass”) is placed at this input node to replicate a fixed-base boundary condition as is present on the shaker table and allow the application of acceleration boundary conditions.

Using the measured acceleration data, $\vec{a}^{(i)}(t)$, the three translational and three rotational accelerations at the seismic mass can be estimated. The acceleration at one of the measurement locations, $\vec{x}^{(i)}$, is a combination of the translational motion and the rotation motion of the base of the structure and can be represented as

$$\vec{a}^{(i)}(t) = \vec{A}(t) + \vec{\alpha}(t) \times \vec{r}^{(i)} \quad (1)$$

where $\vec{A}(t)$ is the translational acceleration at $\vec{x}^{(0)}$, $\vec{\alpha}(t)$ is the rotational acceleration at $\vec{x}^{(0)}$, and $\vec{r}^{(i)}$ is the moment arm from $\vec{x}^{(0)}$ to $\vec{x}^{(i)}$ computed as

$$\vec{r}^{(i)} = \vec{x}^{(i)} - \vec{x}^{(0)}. \quad (2)$$

These quantities are depicted in **Error! Reference source not found.**.

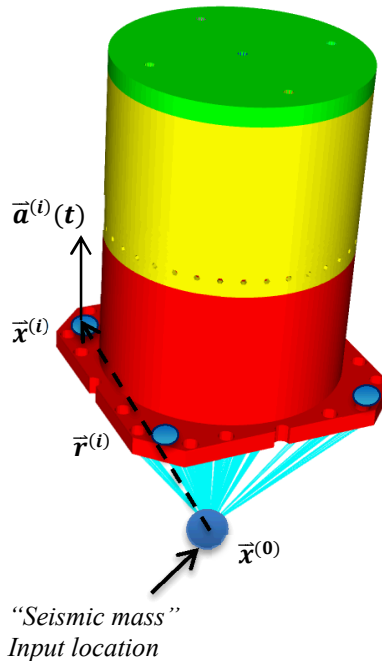


Figure 6 – Model setup showing “seismic mass” location $\vec{x}^{(0)}$, accelerometer measurement locations $\vec{x}^{(i)}$, and acceleration measurements $\vec{a}^{(i)}(t)$. The moment arm from the seismic mass to the accelerometer locations is shown as $\vec{r}^{(i)} = \vec{x}^{(i)} - \vec{x}^{(0)}$.

In matrix form, equation (1) can be written as

$$\{a(t)\} = \{A(t)\} + [\tilde{r}]^T \{\alpha(t)\} \quad (3)$$

where the matrix $[\tilde{r}]$ is defined as the skew-symmetric matrix

$$[\tilde{r}] = \begin{bmatrix} 0 & -r_z & r_y \\ r_z & 0 & -r_x \\ -r_y & r_x & 0 \end{bmatrix}. \quad (4)$$

Here, r_x , r_y , and r_z are the components of the vector $\vec{r}^{(i)}$ at measurement location i .

Application of equation (3) at each measurement location and combining yields the set of equations

$$\begin{Bmatrix} a^{(1)}(t) \\ a^{(2)}(t) \\ \vdots \\ a^{(n)}(t) \end{Bmatrix} = \begin{bmatrix} [I] & [\tilde{r}^{(1)}]^T \\ [I] & [\tilde{r}^{(2)}]^T \\ \vdots & \vdots \\ [I] & [\tilde{r}^{(n)}]^T \end{bmatrix} \begin{Bmatrix} A(t) \\ \alpha(t) \end{Bmatrix}. \quad (5)$$

Here $[I]$ is the three-by-three identity matrix. Solution of equation (5) for $\begin{Bmatrix} A(t) \\ \alpha(t) \end{Bmatrix}$ yields the desired translational and rotational inputs for the model. These time-domain quantities were used directly for the shock calculations presented below. For the random vibration simulations, the time histories are used to compute a six-by-six input power spectral density (PSD) matrix $[S(f)]$. The response of the structure is then computed as

$$[G(f)] = [H(f)][S(f)][H(f)]^*, \quad (6)$$

where $[H(f)]$ is the complex transfer function matrix between the input location, $\vec{x}^{(0)}$, and any desired output response locations on the structure. The $*$ represents the complex conjugate.

6 DOF ANALYSIS WORKFLOW & CONSIDERATIONS

During testing, acceleration time histories from the primary axes (X , Y , and Z) were obtained for accelerometers mounted at the base of the test article. The coordinates of these accelerometers must be measured relative to the location of the “seismic mass” in the model. This data serves as input to the 6 DOF toolkit as shown in Figure 7. This analysis workflow automates much of the theory and considerations discussed in the “Derivation of 6 DOF Model Input” section above. Outputs of the toolkit are function files for a 6x6 PSD input for random vibration analysis or 6 transient input signals for shock analysis. PSDs or shock response spectra (SRS) are also calculated depending on the type of analysis to be performed. Output function files are readily deployed in the Sierra Mechanics analysis suite to be applied to the seismic mass using the modeling approach discussed in the “Configurations” section. This basic procedure was performed for all of the 6 DOF and 1 DOF tests of interest in the current study.

Some unique considerations are necessary for derivation of 6 DOF analysis input from test data. First the time series of accelerometer data must be recorded. This is common in shock testing, but often only PSDs are recorded for vibration testing. Furthermore, an accurate description of accelerometer locations is needed to derive rotational

inputs. Knowledge of accelerometer polarity is crucial for deriving 6 DOF inputs using consistent measurements. The 6 DOF toolkit has troubleshooting features to aid the analyst in accounting for these unique considerations.

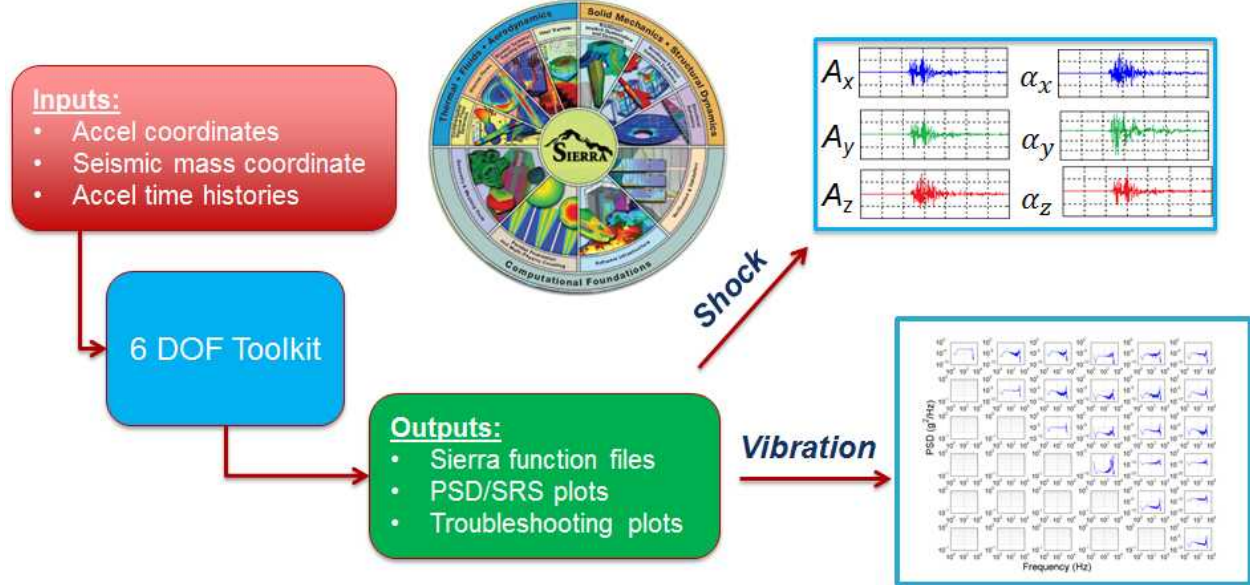


Figure 7 – 6 DOF analysis workflow.

RANDOM VIBRATION ANALYSIS

The model described in the “Configuration” section was considered for modal random vibration analysis using Sandia’s Sierra Mechanics code suite [16,17]. Full 6 DOF inputs for both 6 DOF and 1 DOF testing were derived using the theory and workflow described in previous sections. A modal resolution up to 4 kHz was employed and modal damping of 2% was specified. This modal resolution minimized modal truncation up to the 2 kHz frequency band of interest for vibration analysis.

First, the Z axis testing is considered for both 1 DOF and 6 DOF shakers. During the test on the 1 DOF shaker only the primary axis (Z) can be controlled. This results in off-axis inputs (X and Y) producing unpredictable levels dictated by modes of the test article and table. Figure 8 shows a comparison of the X, Y, and Z input levels for the 1 and 6 DOF testing of a primarily Z input test. Recall that the 6 DOF test control algorithm sought off-axis input levels one order of magnitude lower than the primary Z axis signal while minimizing coherence between in and off-axis input signals. Coherence provides an estimate of the causality between two signals. Thus, minimizing coherence between in and off-axis input signals should result in a primarily single-axis test input.

Inspection of Figure 8 shows that although the 1 DOF test provides very good control of the Z input signal, the level of the off-axis signals can vary significantly over the test frequency band. Off-axis input levels can become significant at higher frequencies where modes of the test article and table may be interacting. The 6 DOF shaker also minimizes coherence between in-axis (Z) and off-axis (X) inputs. Although off-axis terms of the 6 DOF shaker are consistently controlled across the test frequency range, off-axis levels are often higher than those for the 1 DOF shaker. Depending on the application, this predictability in test input may be preferable even if it results in higher off-axis input levels at some frequency bands.

In addition to the primarily Z input test, 6 DOF tests were also performed with significant levels in all translation al DOF (with rotational inputs minimized) and significant levels in all 6 DOF inputs. Figure 9 presents root mean square (RMS) von Mises stress contours for all input cases considered in the test matrix shown in Table I. Clearly there are different stress distributions and levels for each test scenario, indicating the sensitivity of a test article's stress state to single and 6 DOF vibration testing. The degree of sensitivity, however, will be dictated by the modal characteristics of a particular test article and the input profiles.

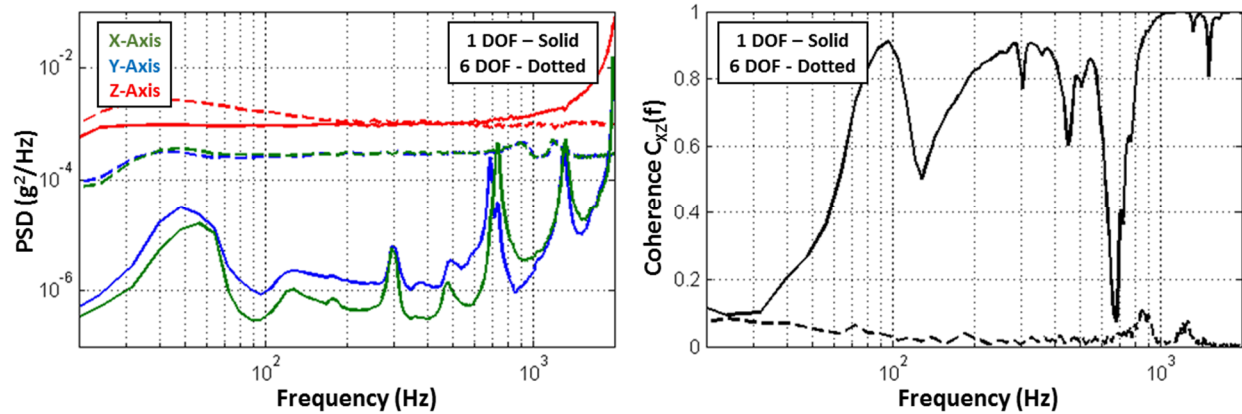


Figure 8 – Typical PSD and coherence plots for the Z-input experimental test on both 6 DOF and 1 DOF shakers.

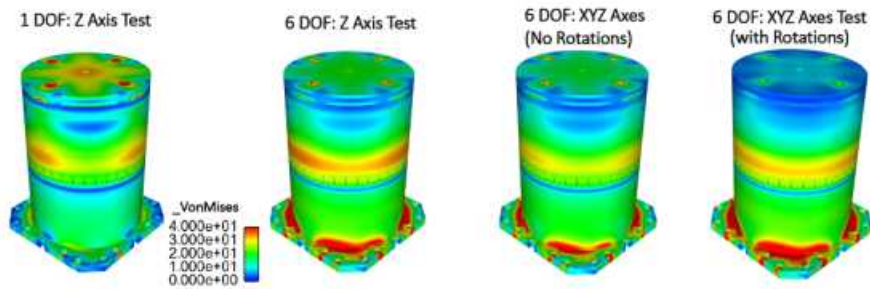


Figure 9 – Calculated RMS von Mises stress for each of the different random vibration tests (contours scaled from 0-40 psi).

SHOCK ANALYSIS

Shock analysis of the model described in the “Configuration” section was considered using the modal transient solution case in Sandia’s Sierra Mechanics code suite [16,17]. This method uses a reduced order model with a subset of modes for efficient transient analysis. A modal resolution up to 7 kHz was employed for modal transient analysis and modal damping of 2% was specified. This resolution was adequate to minimize modal truncation effects for all

environments considered for shock analysis. Transient analysis used the Newmark-Beta implicit time integration method with a time step of 8.3e-5 seconds. This time step was consistent with input the input signal discretization and is expected to provide good temporal resolution for stress predictions.

The input for shock analysis considered a 6 DOF input that was derived from measurements during an operational environment the test article will be exposed to during its life-cycle. Single-axis inputs of the environment (applying only the derived X, Y, or Z inputs) were also considered. See Figure 10 for an illustration of input signals.

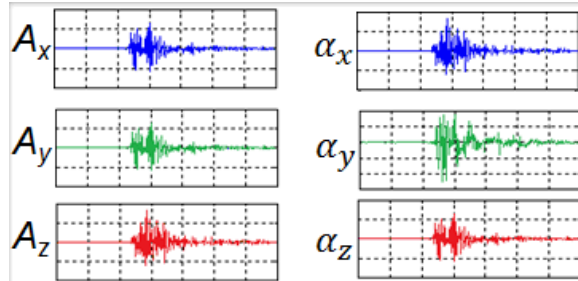


Figure 10 – Illustration of 6 DOF inputs derived from operational environment.

The von Mises stress history in the model was examined for the case of 6 DOF and single axis inputs in X, Y, and Z respectively. Snapshots of stress contours were taken at the time of peak stress and compared between the various simulations as shown in Figure 11. This comparison clearly illustrates the difference in stress states between 6 DOF and 1 DOF input. The 6 DOF shock analysis was also compared to a 3 DOF analysis that applied all translational inputs, but no rotational inputs. Stress contours of this comparison are shown in Figure 12. Although stress contours are more comparable than those in the 6 to 1 DOF input comparison, the effect of rotational inputs on stress is clear. Indeed, if one examines structural matrices a significant portion of the terms are related to rotational degrees of freedom. The importance of rotational effects, however, will be dependent on the input signals and system of interest.

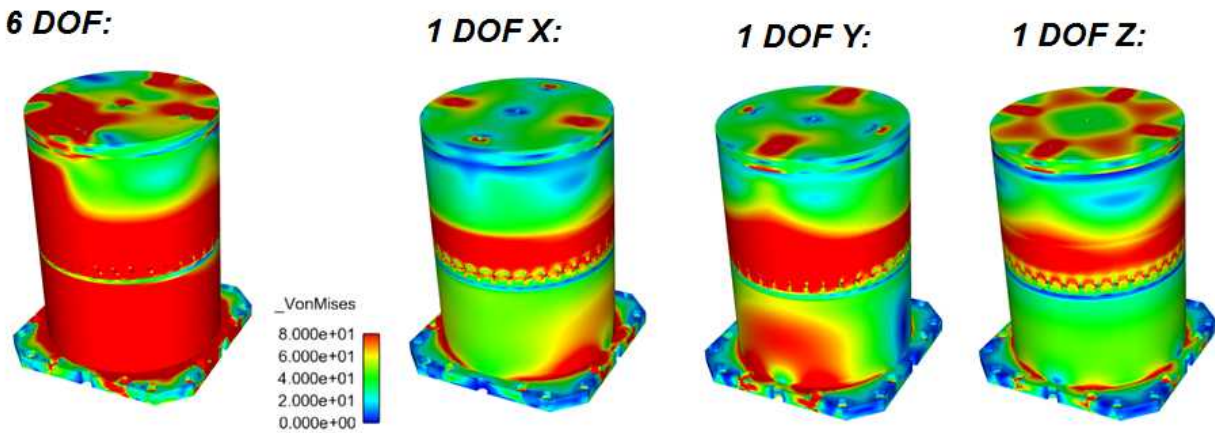


Figure 11 – Comparison of stress contours for 6 DOF and single-axis inputs (contours scaled from 0 -80 psi).

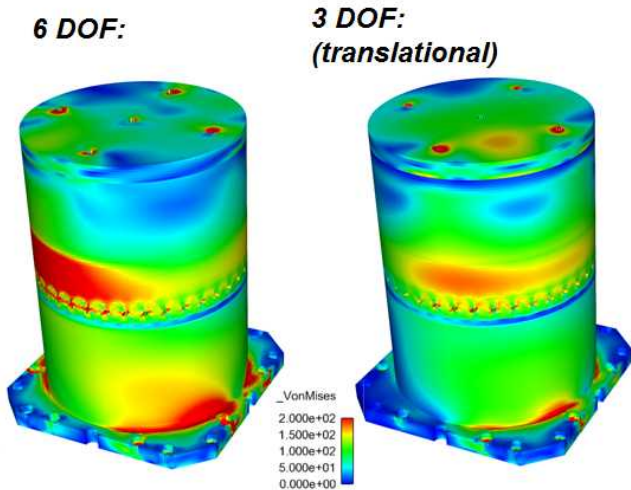


Figure 12 – Comparison of stress contours for 6 DOF and 3 DOF inputs (contours scaled for 0-200 psi).

CONCLUSIONS

This paper has presented a study of 6 degree of freedom testing and analysis. 6 DOF testing affords design and qualification programs the opportunity to consider multi-axis test environments that are more representative of a true operational environment. 6 DOF testing hardware also allows for traditional 1 DOF test approach to be improved by exercising control over off axis inputs. These aspects of 6 DOF testing allow for a more representative stress state to be excited in a test article during mechanical shock and vibration environments. Thus, 6 DOF testing has the potential to facilitate higher performance designs and qualification programs with lower conservatism and lower risks.

6 DOF analysis complements 6 DOF testing by providing greater insight into the effect of multi-axis testing on a test article and can be used as a tool for developing improved testing methodologies. Characterization of a multi-axis test input also reduces uncertainty during model validation/calibration exercises and improves the predictive capability of a model. The authors have developed a toolkit to streamline 6 DOF analysis and continue to gain insight into 6 DOF testing through analytical investigations.

Vibration testing showed clear differences in input characteristics and test article response for 1 and 6 DOF testing. 6 DOF testing allows a test engineer to minimize coherence between in- and off-axis inputs, thereby maintaining better control of input and test article response when applying conventional single-axis test specification. Analytical 6 DOF vibration studies examined the stress response in a test article under various multi-axis and single-axis inputs. Future work will seek to gain a better understanding of the interplay of coherence and off-axis test level control during 6 DOF testing and the influence these factors have on test article response.

Shock analysis examined the response of a test article under 6 DOF input obtained from measurements during an operational environment and a single-axis input broken out from 6 DOF measurements. This study provided a comparison of improved 6 DOF testing/analysis methodologies to traditional single-axis approaches. Results showed a clear difference in stress response between 6 DOF and single axis input, indicating the significant of accounting for multi-axis inputs during test and analysis activities. A subsequent study confirmed the importance of including rotational inputs in addition to translational inputs.

ACKNOWLEDGEMENTS

The authors wish to acknowledge Dr. Laura Jacobs-O'Malley, Dr. Garrett Nelson, and Mr. John Hofer of the Vibration and Acoustic Simulation Department at Sandia National Laboratories for performing the experimental activities described in this paper.

REFERENCES

1. U.S. Department of Defense Environmental Engineering Considerations and Laboratory Tests, MIL-STD-810G, Oct. 2008.
2. U.S. Navy Manufacturing Screening Test Standards, NAVMAT P-9492, May 1979.
3. JEDEC Standard: Vibration Variable Frequency, JESD22-B103B, Jun. 2006.
4. D.L. Gregory, F. Bitsie, and D.O. Smallwood, "Comparison of the response of a simple structure to single axis and multiple axis random vibration inputs," in Proc. 80th Shock and Vibration Symp., San Diego, CA, Oct. 2009.
5. R.M. French, R. Handy, and H.L. Cooper, "A comparison of simultaneous and sequential single-axis durability testing," Experimental Techniques, vol. 30, no. 5, pp. 32-7, Sept./Oct. 2006.
6. W.E. Whiteman and M.S. Berman, "Fatigue failure results for multi-axial versus uniaxial stress screen vibration testing," Shock and Vibration, vol. 9, no. 6, pp. 319-28, 2002.
7. H. Himelblau et al., "Effects of triaxial and uniaxial random excitation on the vibration response and fatigue damage of typical spacecraft hardware" in Proc. 66th Shock and Vibration Symp., Arlington, VA, Oct. 1995.
8. C. Peterson, "Time-to-failure testing using single- and multi-axis vibration," Sound and Vibration, vol. 47, no. 3, pp.13-7, Mar. 2013.
9. M.T. Freeman, "3-Axis vibration test system simulates real world," TEST Eng. and Manage., pp. 10-14. Dec./Jan. 1990-1991.
10. J. Hoksbergen, "Advanced high-frequency 6-DOF vibration testing using the Tensor," Sound and Vibration, vol. 47, no. 3, Mar. 2013.
11. D.J. Osterholt, N.C. Yoder, and D. Linehan, "Advances in six degree of freedom vibration testing," in Proc. Experimental and Appl. Mechanics, Jun. 2007.
12. Team Corporation, "Tensor 900 multi-axis high frequency vibration test system," [Online]. Available: http://www.teamcorporation.com/images/brochures_A4/Tensor900_A4.pdf
13. D.O. Smallwood and D.L. Gregory, "Evaluation of a 6-DOF electrodynamic shaker system," in Proc. 79th Shock and Vibration Symp., Orlando, FL, Oct. 2008.
14. M.A. Underwood and M. Hale, "MIMO testing methodologies," in Proc. 79th Shock and Vibration Symp., Orlando, FL, Oct. 2008.
15. B.R. Pacini and D.G. Tipton, "Structural-acoustic mode coupling in a bolted aluminum cylinder," in Proc. 34th IMAC Conference and Exposition on Structural Dynamics., Orlando, FL, Jan. 2016.
16. Sierra Structural Dynamics Development Team, *Sierra/SD – Theory Manual*, SAND 2011-8272, Sandia National Laboratories, Albuquerque, New Mexico, April 2015.
17. Sierra Structural Dynamics Development Team, *Sierra Structural Dynamics-User's Notes*, Sandia National Laboratories, Albuquerque, New Mexico, April 2015.